NEW γ-RAY SCANNER FOR TRACKING ARRAYS*

Katyayni Tiwari[a], Arzoo Sharma[a], J. Gerl[b], I. Kojouharov[b]
P. Herrmann[b], H. Schaffner[b], G. Aggez[c], H.M. Albers[b]
T. Habermann[b], Biswarup Das[b], Pushpendra P. Singh[a]

[a]Indian Institute of Technology Ropar, Rupnagar — 140 001, Punjab, India
[b]GSI Helmholtzzentrum für Schwerionenforschung
Darmstadt 64291, Germany
[c]Istanbul University, Department of Physics
Istanbul 34116, Turkey

Received 27 November 2023, accepted 17 January 2024,
published online 24 April 2024

In recent years, a great deal of effort has been devoted to developing arrays of highly segmented germanium detectors, signal-processing electronics, and γ-ray tracking algorithms. With this advancement, the interaction points associated with a particular γ-ray can be identified in terms of spatial coordinates and deposited energy. The tracking provides the direction of the γ-ray emission and the position of its first interaction inside the detector. The detectors have a complex geometry and require sophisticated characterization/scanning systems. The prime objective of the present work is to improve the GSI 3D scanning system, particularly regarding position detector readout, its resilience, and speed, allowing for faster scanning of the entire segmented detector. In the proposed advancement, Silicon PhotoMultiplier (SiPM), *i.e.*, an array of square Avalanche PhotoDiodes, is employed to replace the previous position-sensitive Photo Multiplier Tube. A scanning device using a LYSO scintillator crystal coupled to an array of 96 position-sensitive SiPMs has been developed and coupled with a GSI-developed electronics TAMEX system. Before scanning any segmented detector, the scanner has been fully characterized. The work presents preliminary results of the performance evaluation and characterization of the new γ-ray scanner at GSI, Germany.

DOI:10.5506/APhysPolBSupp.17.3-A15

1. Introduction

The γ-ray spectroscopy, with the introduction of highly segmented position-sensitive germanium detectors, has seen significant advancements in

* Presented at the XXXVII Mazurian Lakes Conference on Physics, Piaski, Poland, 3–9 September, 2023.

the last decades [1]. One notable example of such advanced detectors is the Advanced GAmma-ray Tracking Array (AGATA) [2], a consortium project of 13 European countries, developed for high-resolution γ-ray spectroscopy. These detectors have remarkable characteristics enabling γ-ray tracking based on Pulse Shape Analysis (PSA) [3]. γ-ray tracking within segmented detectors involves analyzing trajectories of individual γ-rays as they traverse the detector, providing information on their origin, direction, energy, and interaction location [4, 5]. To obtain this information, the response of the detector to γ-rays needs to be well understood. In order to characterize a detector, a database of pulse shapes can be developed through simulations and experimental measurements. A complete PSA algorithm analyzes signals from detector's segments, providing information on the number of γ-ray interactions, spatial coordinates of these points, and energy deposition, which aids in understanding γ-ray behavior within the crystal. Due to the complexity of the detector geometries, maintaining a database of pulse shapes is crucial for comprehending the operation of detectors and their behavior under various experimental conditions. Thus, dedicated scanning systems have been developed by different groups. One such scanning system is the Liverpool scanner, consisting of a scanning table and a collimated source, as discussed in Ref. [6]. Another state-of-the-art scanner, a one-shot scanning device, has been developed at GSI Helmholtzzentrum für Schwerionenforschung, Germany [7]. It uses a fast scanning technique that does not require source collimation. Further, within the NuSTAR Collaboration, the Indian Institute of Technology Ropar together with GSI, Germany has developed a new detector scanning system. This scanning system combines sophisticated pulse shape analysis algorithms with γ-ray imaging techniques. It is based on the principle of pulse shape comparison and positron annihilation correlation [8–11]. Two orthogonal sets of pulse shapes are compared in order to determine the pulse for a particular position [12]. The first measurements aiming at characterization of the newly developed detector have been carried out using the GSI scanning facility. The experiment and its results are described in detail in the following sections.

2. Experimental details

The new Position-Sensitive Detector (PSD) consists of a cylindrical cerium-doped Lutetium Yttrium OrthoSilicate (LYSO) scintillator crystal with dimensions of 7 cm (diameter) $\times$ 3 mm (thickness). The selection of the scintillator is based on its properties: (a) efficient conversion of γ-ray energy to light, (b) complete stopping, and (c) fast-time response. The cerium-doped lutetium scintillator crystals are widely used for various applications, such as high-energy physics, PET imaging, *etc.* This material contains ^{176}Lu,

which is radioactive. The scintillator was coupled to the matrix of 96 Sensl-manufactured c-type 3 mm × 3 mm Silicon Photomultipliers (SiPMs) using RTV615 silicone compound-based optical glue. SiPMs are pixelated photodetectors widely used in nuclear and medical physics due to their fast response time and compact size [13–15]. The array has been constructed on a PCB with a back end containing an RC circuit for pulse readout. Figure 1 (a) shows the scintillator coupled to the SiPM matrix. The output was taken from the p-side (anode), implying negative biasing to the detector for reverse biasing conditions. The characterization has been performed, establishing the coincidence between the GSI scanner and the PSD. The scanning setup consists of a PSD with a ^{22}Na source and a Position-Sensitive Photo-Multiplier Tube (PSPMT) connected to a LYSO crystal. The PSPMT has a mesh of 16 X and 16 Y anodes.The spatial resolution of the GSI scanner is approximately 1 mm. Two 511 keV γ-rays are emitted in opposite directions following positron annihilation, which is used to set up the coincidence between the PSD and the GSI scanner.

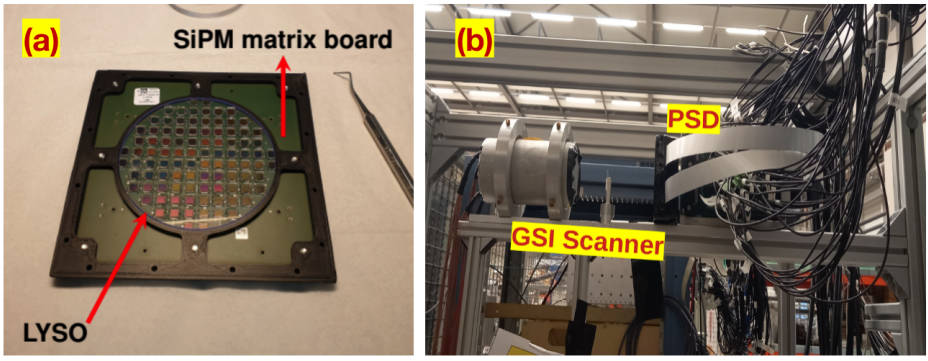

Fig. 1. (a) Photo of the PSD depicting a thin cylindrical LYSO scintillator coupled with the SiPM board. (b) Photo of the coincidence detector setup between the GSI scanner (left) and the PSD (right) with a ^{22}Na source mounted on the aluminium frame of the setup.

The coincidences were demanded between the GSI scanner and the PSD, using the setup presented in Fig. 1 (b). The distance between the ^{22}Na source and the PSD was ≈ 8.2 cm. A VME-based 32-channel QDC was used for the PSPMT readout. For PSD, the detector output was connected to the new FPGA-based advanced digitizer, TAMEX [16, 17]. The newest analog front-end discriminator used with the TAMEX is the "TwinPeaks" card developed at GSI [16, 17]. TwinPeaks can provide signals for both time and energy measurements using two independent branches. Inside the card, the input is split into two branches: (a) fast branch — to measure

the leading edge time of the input signal, and (b) slow branch — for energy measurement. The fast branch provides log amplification for timing, and the slow branch has linear amplification for energy measurement based on the time-over-threshold principle.

3. Analysis and results

A 2D image was reconstructed using the GSI scanner for the coincidence setup. The image depicts a uniform charge distribution for the coincidence data. This measurement was obtained after optimization of threshold settings to achieve the best possible charge distribution. By checking 2D images online using GO4 [18], the distance was optimized for the full solid angle coverage around the PSD. The 2D image obtained from the GSI scanner is shown in Fig. 2 (a). The Position_X and Position_Y have been obtained for the coincidence data using the charge distribution along the x and y axis, respectively, of the photomultipliers of the scanner. A minimum threshold was applied to the Time-Over-Threshold (TOT) spectrum to investigate the amplitude of signals in the neighbouring channels.

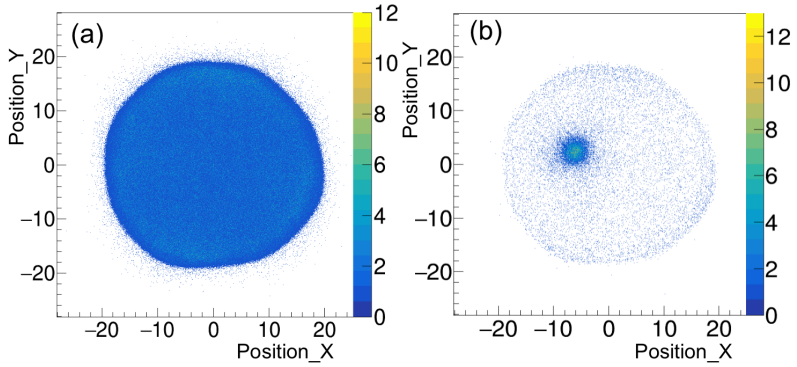

Fig. 2. 2D coincidence image obtained from the scanner for (a) all the channels, (b) one of the central SiPM firing/gated.

The analysis has been extended to study the position response of the PSD using an energy gate applied to one of the SiPMs. The 2D image reconstructed for one of the middle SiPMs is shown in Fig. 2 (b). Later, the 2D image is projected onto the x axis to sub-divide the segment, *i.e.*, to find the detector response to γ-rays with better than 3 mm position sensitivity. The selected SiPM was divided into three sections. For each of the cuts, a 2D image was constructed for the PSD to find the response of the neighboring channels. It is plotted in Fig. 3, where x and y represent the axes of the PSD. In this figure, the reference channel is denoted by n_0, and

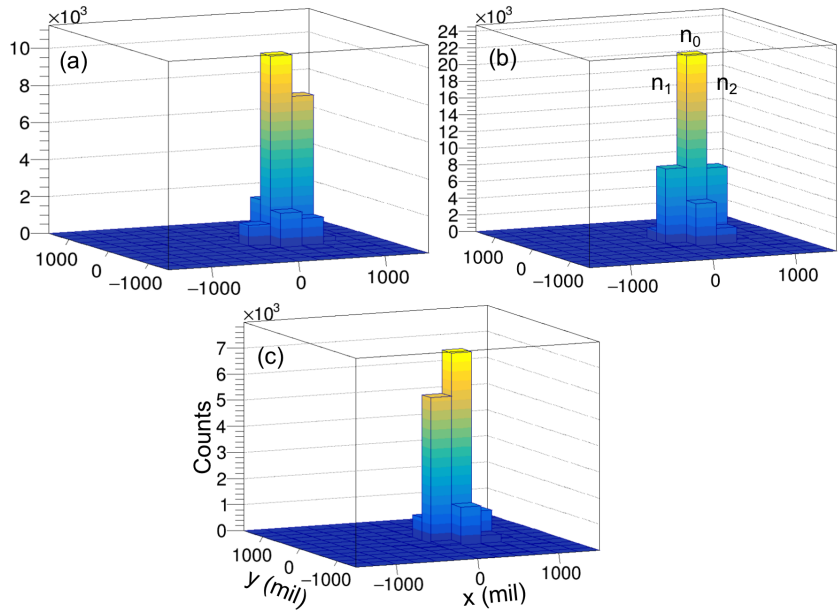

Fig. 3. Intensity distribution plot for the selected/reference SiPM in the PSD, denoted by n_0 (the reference channel), and its immediate neighbors n_1 (left channel) and n_2 (right channel). The x and y axes are positions in mil (1 mil = 0.0254 mm), and the z axis depicts the intensity distribution along these axes. The plots were constructed for a fixed position along y axis and various cuts along the x axis applied to the projected image of Fig. 2 (b). Panels (a), (b), and (c) represent plots obtained from cuts along the right, center, and left, respectively.

the first neighboring channels are n_1 (left) and n_2 (right). The plots have been constructed for a fixed y position and various cuts along the x axis of an X-projected 2D image in Fig. 2 (b), *i.e.*, Fig. 3 (a), (b), and (c) represent cuts along the right, center, and left, respectively. The maximum number of counts corresponds to the n_0 channel, and the left and right channels represent n_1 and n_2, respectively. For the right cut, *i.e.*, in Fig. 3 (a), n_2 is observed to have more counts than n_1. The middle cut has approximately similar intensities for n_1 and n_2, as shown in Fig. 3 (b). A higher number of counts is observed for n_1 for the left cut, represented by Fig. 3 (c). Hence, it is observed that the intensities and/or amplitudes of signals from the neighboring channels are position-sensitive, and the distribution suggests a local γ-ray hit, which may be attributed to the threshold selection. From this preliminary analysis, it is inferred that the detector is position-sensitive to γ-ray hits with a resolution better than 3 mm. A further analysis aims to quantify the position resolution.

4. Summary and conclusions

A new γ-ray scanner has been developed jointly by IIT Ropar and GSI, Germany using an advanced readout technology, being affordable, miniature, compact, and with a good spectral response. This state-of-the-art scanner consists of a cerium-doped LYSO scintillator crystal coupled with a matrix of 96 SiPMs. The testing was performed at GSI, Germany using imaging capabilities with an existing scanner to support the upcoming DESPEC (DEcay SPECtroscopy) experiments [19]. A preliminary qualitative analysis has been performed by investigating the amplitude difference in the neighborhood of the hit channel. The results suggest that a good position resolution can be achieved. Various position reconstruction algorithms will be developed using machine learning to support the present development.

In this work, Katyayni Tiwari and Arzoo Sharma have contributed equally. The authors acknowledge GSI Helmholtzzentrum für Schwerionenforschung, Germany, for generously providing access to their experimental facility, all GSI/DESPEC (DEcay SPECtroscopy) group members for quick help, valuable feedback, and the Indian Institute of Technology Ropar for an ISIRD Grant for the development of the scanner. One of the authors, K.T. thanks the Department of Science & Technology for INSPIRE Fellowship and A.S. acknowledges GSI GET_INvolved/FAIR for financial support.

REFERENCES

[1] J. Eberth, J. Simpson, *Prog. Part. Nucl. Phys.* **60**, 283 (2008).
[2] S. Akkoyun *et al.*, *Nucl. Instrum. Methods Phys. Res. A* **668**, 26 (2012).
[3] R. Venturelli, D. Bazzacco, LNL Annual Report, 2005, 2004.
[4] F.C.L. Crespi *et al.*, *Nucl. Instrum. Methods Phys. Res. A* **570**, 459 (2007).
[5] M. Krammer *et al.*, «Handbook of Particle Detection and Imaging», *Springer*, 2021, pp. 317–352.
[6] M.R. Dimmock *et al.*, *IEEE Transactions on Nuclear Science* **56**, 2415 (2009).
[7] N. Goel, Ph.D. Thesis, 2011.
[8] N. Goel *et al.*, *Nucl. Instrum. Methods Phys. Res. A* **700**, 10 (2013).
[9] T. Habermann *et al.*, *Nucl. Instrum. Methods Phys. Res. A* **873**, 24 (2017).
[10] C. Domingo-Pardo *et al.*, *Nucl. Instrum. Methods Phys. Res. A* **643**, 79 (2011).
[11] N. Goel *et al.*, *Nucl. Instrum. Methods Phys. Res. A* **652**, 591 (2011).
[12] A. Sharma *et al.*, *Nucl. Instrum. Methods Phys. Res. A* **1051**, 168233 (2023).
[13] A. Bornheim *et al.*, *Nucl. Instrum. Methods Phys. Res. A* **896**, 75 (2018).

[14] A.J. González *et al.*, *Nucl. Instrum. Methods Phys. Res. A* **787**, 42 (2015).

[15] M. Benetti *et al.*, *Nucl. Instrum. Methods Phys. Res. A* **658**, 61 (2011).

[16] A. Banerjee *et al.*, *Proc. SPIE* **11494**, 1149405 (2020).

[17] A. Banerjee *et al.*, *Nucl. Instrum. Methods Phys. Res. A* **1028**, 166357 (2022).

[18] `https://www.gsi.de/en/work/research/experiment_electronics/data_processing/data_analysis/the_go4_home_page`, 2023.

[19] A.K. Mistry *et al.*, *Nucl. Instrum. Methods Phys. Res. A* **1033**, 166662 (2022).